Metabolomics
DOI 10.1007/s11306-012-0416-6

ORIGINAL ARTICLE

Metabolome analysis during the morphological transition of *Candida albicans*

Ting-li Han · Richard D. Cannon · Silas G. Villas-Bôas

Received: 31 October 2011 / Accepted: 1 March 2012
© Springer Science+Business Media, LLC 2012

Abstract *Candida albicans* is an opportunistic pathogen of humans with significant mortality in severely immunocompromised patients. The ability to switch from yeast to hyphal morphology and vice versa, in response to various environmental cues, is believed to be a critical virulence factor of this fungus. However, the mechanisms that recognize such environmental signals and trigger the morphological change at a system level are still not clearly understood. Therefore, we have compared the metabolite profiles of *C. albicans* cells growing under different hyphae-inducing conditions to the metabolite profiles of growing yeast cells. Surprisingly our results suggest an overall downregulation of cellular metabolism during the yeast to hyphal morphological transition. Among the metabolic pathways involved in the central carbon metabolism, we have found seventeen that were significantly downregulated in all three hyphae-inducing conditions. This indicates that these central carbon metabolic pathways are likely to be intrinsically involved in the downstream effects of the morphogenetic process.

Keywords *Candida albicans* · Metabolite profiling · Central carbon metabolism · Metabolomics · Filamentous growth · Morphogenesis

T. Han · S. G. Villas-Bôas (✉)
Centre for Microbial Innovation, School of Biological Sciences, The University of Auckland, 3A Symonds Street, Auckland 1142, New Zealand
e-mail: s.villas-boas@auckland.ac.nz

R. D. Cannon
Department of Oral Sciences, University of Otago, Dunedin, New Zealand

1 Introduction

Candida albicans is the major fungal pathogen of humans capable of causing systemic infections in severely immunocompromised patients. The ability to change from yeast to filamentous growth or vice versa, in response to certain environmental cues, enhances *C. albicans* adaptation and survival in the course of infection (Romani et al. 2003). Despite different morphological forms being found during infection, yeast cells are often associated with dissemination through the bloodstream to colonize internal organs (Bendel et al. 2003; Saville et al. 2003), while the filamentous forms are believed to be more suited to penetrate the host mucosa and epidermal surfaces (Rooney and Klein 2002) as well as to escape from macrophages after phagocytosis (Arai et al. 1977; Lorenz et al. 2004).

The morphological transition of *C. albicans* is triggered by various external signals. The yeast-to-hypha transition can be induced by serum, proline, *N*-acetylglucosamine, quorum sensing molecules, some carbon sources, and other cues (Reynolds and Braude 1956; Holmes and Shepherd 1987; Nickerson et al. 2006). Gene knockout mutagenesis, transcriptomic and proteomic studies have proposed that the morphogenetic process in *C. albicans* is mainly controlled by Ras, PKA, MAPK, HOG, and RIM101 signaling pathways, and regulated by Cph1p, Czf1p, Efg1p, Gcn4p, Mig1p, Nrg1p, Rfg1p, Ssn6p, Tec1p, Tup1p, and Ume6p transcription factors (José et al. 1996; Braun and Johnson 1997; Lo et al. 1997; Stoldt et al. 1997; Brown et al. 1999; Feng et al. 1999; Schweizer et al. 2000; Kadosh and Johnson 2001; Murad et al. 2001; Tripathi et al. 2002; Hwang et al. 2003; Bensen et al. 2004; Maidan et al. 2005a; Banerjee et al. 2008; Han et al. 2011). Relatively little is known, however, about the downstream molecular

Published online: 24 March 2012

effects of these signaling pathways on the primary cell metabolism that result in the morphological transition.

When the yeast-to-hypha transition is triggered upon phagocytosis of *C. albicans* by neutrophils or macrophages, there is evidence that genes involved in glycolysis are immediately down-regulated while those in the glyoxylate cycle, gluconeogenesis and β-oxidation pathways are upregulated (Rubin-Bejerano et al. 2003; Lorenz et al. 2004; Fradin et al. 2005; Fernández-Arenas et al. 2007). Since all these upregulated pathways are involved in the catabolism of non-fermentable carbon sources, the *C. albicans* cells appear to undergo carbon starvation when engulfed by macrophages or neutrophils. Other studies show that this upregulation of catabolic pathways not only allows *C. albicans* to survive in an environment with poor carbon sources, it may also affect the morphogenetic process. For example, a key intermediate in the metabolism of non-fermentable carbon sources is acetyl-CoA. When genes encoding enzymes involved in the biosynthesis, or intracellular shuttle, of acetyl-CoA are deleted, such as acetyl CoA synthase (*ACS2*) and carnitine acetyltransferase (*CTN1*, *CTN2, CAT2*), the resulting mutants are unable to utilize non-fermentable carbon sources such as lactate, acetate, or ethanol as a sole carbon source (Carman et al. 2008; Zhou and Lorenz 2008). The mutants lacking *CTN3* and *CAT2* also demonstrate reduced hyphal formation (Prigneau et al. 2004; Strijbis et al. 2008). Furthermore, *C. albicans* mutants incapable of metabolizing trehalose, galactose, glycerol, or fructose as sole carbon sources are also unable to form hyphae under hyphal-inducing conditions (Zaragoza et al. 1998; Pedreño et al. 2004; Singh et al. 2007). Despite these studies showing the importance of central carbon metabolism to the morphogenetic process, the over-arching changes in the primary metabolism of *C. albicans* in response to morphogenesis-inducing cues have not been studied.

Metabolomics and fluxomics are the most appropriate approaches to investigate the global changes in the central carbon metabolism of *C. albicans* during morphogenesis. Metabolomics, the latest addition of functional genomics tools, aims at analyzing all low-molecular weight compounds produced or modified by a biological system (Villas-Bôas et al. 2005a). Metabolites are not gene products, but their concentrations are affected by the activities of gene products (enzymes) and the availability of precursors (Villas-Bôas et al. 2007). Because signaling can use existing receptors and enzymes to change fluxes within a rigid metabolic network (Raamsdonk et al. 2001), the metabolome responds more rapidly to environmental changes than the transcriptome and proteome. For example, when a glucose-limited culture of *Saccharomyces cerevisiae* is perturbed by glucose, a distinct change of glycolytic metabolite levels can be observed within 3 s after glucose addition (Visser et al. 2004), whilst the first significant change in gene expression is visible only after 2 min (Kresnowati et al. 2006). The metabolome is also expected to amplify the changes occurring in the transcriptome and in the proteome (Kell et al. 2005). Furthermore, the morphogenesis of *C. albicans* is strongly influenced by metabolites such as farnesol, tyrosol, phenylethyl alcohol, tryptophol, estradiol, dodecanol, and different types of carbon and nitrogen sources (Lingappa et al. 1969; Holmes and Shepherd 1987; Hornby et al. 2001; Oh et al. 2001; Chen et al. 2004; Hogan et al. 2004; Maidan et al. 2005b; Cheng et al. 2006). Thus, the study of changes in the metabolome in response to environmental signalling has great potential to assist in the elucidation of the fungal morphogenetic process.

Therefore, we have compared the intracellular and extracellular metabolite profiles of *C. albicans* cells growing under different hyphae-inducing conditions to the metabolite profiles of growing yeast cells using GC–MS based metabolomic methods.

2 Methods

2.1 The rationale behind our experimental design

The metabolite levels of microbial cells will change according to environmental conditions and medium composition. Likewise, *C. albicans* morphogenesis is regulated by environmental conditions and medium composition. Therefore, the challenge for our metabolomics study of *C. albicans* morphogenesis was to differentiate changes in metabolite levels resulting from environmental changes from those changes associated specifically with the morphogenetic process. Thus, we chose to fix the key environmental conditions such as pH, temperature and aeration, and vary the composition of the media to induce morphogenesis. Indeed we used three different hyphae-inducing media and compared each to cells growing in two different media where the yeast form was maintained. Although many changes in the metabolite profile of the cells were related to the different medium compositions, we were able to identify common trends observed in all hyphae-inducing conditions that were independent of the growth media.

2.2 Chemicals

Methanol, chloroform, sodium bicarbonate, and sodium hydroxide were obtained from Merck (Damstadt, Germany). The internal standard 2,3,3,3-d_4-alanine, the derivatization reagent methylchloroformate (MCF), and pyridine were purchased from Sigma-ALdrich (St. Louis, USA). Anhydrous sodium sulphate was obtained from Fluka (Steinheim,

Germany). All chemicals used in this study were of analytical grade.

2.3 Fungal strain and culture media

C. albicans strain SC5314 (Gillum et al. 1984) was maintained on YPD containing yeast extract (6 g L^{-1}), peptone (3 g L^{-1}), glucose (10 g L^{-1}), and agar (15 g L^{-1}) and incubated at 30 °C. Pre-inocula were prepared in YPD broth medium, with the same composition as the agar plates, but without agar. Five different culture media were used for the metabolomic study: (1) minimum mineral medium (MM medium) at pH 6.5 containing D-glucose (10 g L^{-1}), $(NH_4)_2SO_4$ (5 g L^{-1}), $MgSO_4 \cdot 7H_2O$ (0.5 g L^{-1}), KH_2PO_4 (3 g L^{-1}), vitamins and trace metals as previously described (Verduyn et al. 1992); (2) YPD broth medium at pH 6.5 containing yeast extract (6 g L^{-1}), peptone (6 g L^{-1}), and glucose (10 g L^{-1}); (3) minimal-proline and *N*-acetylglucosamine medium (MPA medium), which was the same as the MM medium described above without D-glucose, but supplemented with L-proline (10 mM) and *N*-acetylglucosamine (2.5 mM) at pH 6.5; (4) serum medium, which was MM medium without D-glucose, supplemented with bovine serum (10 % v/v) at pH 6.5; and (5) Lee's medium at pH 6.5 containing D-glucose (12.5 g L^{-1}), $(NH_4)_2SO_4$ (5 g L^{-1}), $MgSO_4 \cdot 7H_2O$ (0.2 g L^{-1}), KH_2PO_4 (2.5 g L^{-1}), NaCl (5.0 g L^{-1}), alanine(0.5 g L^{-1}), leucine (1.3 g L^{-1}), lysine (1.0 g L^{-1}), methionine (0.1 g L^{-1}), phenylalanine (0.5 g L^{-1}), proline (0.5 g L^{-1}), threonine (0.5 g L^{-1}), and biotin (0.001 g L^{-1}) (Lee et al. 1975).

2.4 Yeast and hyphal growth conditions

C. albicans was cultured in 1.4 L of YPD at 30 °C using shake flasks in a rotary shaker overnight. The cells were collected by centrifugation at 2,000*g* (4 °C) for 5 min and washed in phosphate buffered saline (8 g L^{-1} NaCl, 0.2 g L^{-1} KCl, 1.44 g L^{-1} Na_2PO_4, 0.24 g L^{-1} KH_2PO_4, at pH 7.5). The cells were resuspended in the five different growth media described above (MM, YPD, MPA, serum, and Lee's media) to an initial OD_{600} of 0.5. The cell suspensions were incubated using shake flasks in a rotary shaker-incubator at 37 °C for 3 h. The morphology of *C. albicans* in each growth medium was monitored using a phase contrast microscope (DMR, Lecia).

2.5 Sampling and quenching of cell metabolism

Five shake-flasks containing 100 mL of culture from each growth medium were harvested at time zero (right after resuspension), and after 1, 2, and 3 h incubation. For intracellular metabolite analysis, 90 mL of the cultures were rapidly filtered under vacuum (Air Cadet vacuum/pressure station, Thermo), quickly washed with cold saline solution (1–2 °C) and quenched in cold methanol water (50 % v/v) at −30 °C as described by Smart et al. (2010). The remaining 10 mL of microbial cultures were filtered through syringe filters (0.2 µm pore size) to remove the microbial cells, and the filtrate was used for the analysis of extracellular metabolites.

2.6 Sample preparation for metabolite analysis

The intracellular metabolites were extracted from the quenched cell pellets using cold methanol water and freeze–thaw cycles following the protocol described by Smart et al. (2010). The Internal standard 2,3,3,3-d_4-alanine (0.3 µmol/sample) was added to each sample before extraction. The intracellular metabolite extracts and 1 mL of spent culture medium containing extracellular metabolites were freeze-dried (BenchTop K manifold freeze dryer, VirTis) before chemical derivatization.

2.7 Chemical derivatization of metabolites

The freeze-dried samples were derivatised using the methyl chloroformate (MCF) method according to the protocol described by Smart et al. (2010). In summary, the freeze-dried samples were resuspended in 200 µL of sodium hydroxide solution (1 M) and transferred to silanised glass tubes, then mixed with 167 µL of methanol and 34 µL of pyridine. The derivatisation began by adding 20 µL of MCF followed by vigorously mixing for 30 s, and then a further 20 µL of MCF was added followed by vigorously mixing for 30 s. To separate MCF derivatives from the reactive mixture, 400 µL of chloroform was added and vigorously mixed for 10 s followed by the addition of 400 µL of sodium bicarbonate solution (50 mM), and mixing for an additional 10 s. The aqueous layer was removed and dehydrated with anhydrous sodium sulphate before samples were transferred to GC–MS vials.

2.8 Gas chromatography–mass spectrometry (GC–MS) analysis

The MCF derivatives were analysed in an Agilent GC7890 system coupled to a MSD5975 mass selective detector (EI) operating at 70 eV. The column used for all analyses was a ZB-1701 GC capillary column (30 m × 250 µm id × 0.15 µm with 5 m guard column, Phenomenex). The analysis parameters were set according to Smart et al. (2010). Samples were injected under pulsed splitless mode with the injector temperature at 290 °C. The helium gas flow through the GC-column was set at 1.0 mL min^{-1}. The GC-oven temperature was initially held at 45 °C for 2 min.

Then the temperature was raised with a gradient of 9 °C.min^{-1} until it reached 180 °C and was held for 5 min. Then the temperature ramped at 40 °C.min^{-1} until it reached 220 °C and was held for 5 min. Then the temperature was ramped at 40 °C.min^{-1} until it reached 240 °C and was held for 11.5 min. Lastly, the temperature was ramped at 40 °C.min^{-1} until it reached 280 °C and was held for 2 min. The interface temperature was set to 250 °C and the quadrupole temperature was 200 °C.

2.9 Biomass quantification

The cell debris collected after intracellular metabolite extraction was dried by using a microwave (250 W for 20 min) and weighed in order to estimate the biomass (dry weight) content of each sample.

2.10 Data mining, data normalization, and data analysis

AMDIS software was used for deconvoluting GC–MS chromatograms and identifying metabolites using an in-house MCF mass spectra library. The identifications were based on both MS spectrum of the derivatised metabolite and its respective chromatographic retention time. The relative abundance of identified metabolites was determined by ChemStation (Agilent) by using the GC base-peak value of a selected reference ion. These values were normalised by the biomass content in each sample as well as by the abundance of internal standard (2,3,3,3-d_4-alanine). A univariate analysis of variance (ANOVA) was applied to determine whether the relative abundance of each identified metabolite was significantly different between growth conditions. Our Pathway Activity Profiling (PAPi) algorithm (Aggio et al. 2010) was used to predict and compare the relative activity of different metabolic pathways in *C. albicans* during the growth conditions tested. This programme connects to the KEGG online database (http://www.kegg.com) and uses the number of metabolites identified from each pathway and their relative abundances to predict which metabolic pathways are likely to be active in the cell. The entire data mining, data normalisation and pathway activity predictions were automated in R software as described by Smart et al. (2010) and Aggio et al. (2010).

2.11 Quantification of intracellular ATP pools

The intracellular pool of ATP was determined by using the luminescence ATP detection assay ATPlite™ (PerKinElmer). This assay measures light emission caused by the enzymatic reaction between ATP and luciferin-luciferase. Media without cells were used to determine the assay background signal for each medium. Three technical replicates of 100 µL culture were collected from each flask ($n = 5$) after 3 h of incubation. The cells were lysed and the total ATP content was quantified according to the manufacturer's instructions using ATP standard curves obtained from media spiked with ATP standard solutions (one calibration curve for each medium). Light emission was measured using a bioluminescence plate reader (Envison™, PerkinElmer).

3 Results

3.1 Hyphae-induction in *C. albicans*

To study the metabolomic changes associated with *C. albicans* morphogenesis, we cultivated *C. albicans* in three different hyphae-inducing media (MPA, serum, and Lee's) for three hours and compared their morphology to cells grown in yeast form in two different media (MM and YPD). Microscopic examination revealed that at least 95 % of cells developed hyphae in hyphae-inducing media. Some pseudohyphae (thick hyphae with constrictions at the septa or chains of elongated yeast cells) were also present in Lee's medium. On the other hand, approximately 100 % of cells maintained the yeast form in MM and YPD media after three hours incubation (Fig. 1; Table 1). We observed a significant increase in the biomass of C. *albicans* cultures growing in serum, Lee's, and YPD media, whilst the cultures growing in MM, or MPA media showed just a small increase in biomass during three hours of incubation. This was expected since bovine serum, YPD broth, and Lee's medium, unlike the other media, contained several free amino acids and peptides that are easily metabolised, promoting faster growth (Eisman et al. 2006).

3.2 The metabolite profile of *C. albicans* during morphogenesis

We detected over a hundred GC–MS peaks in *C. albicans* intracellular samples, and seventy-five of them were identified using our in-house MCF MS library (Table 2). Metabolites identified included a range of intermediates from central carbon metabolism, such as phosphoenolpyruvate, pyruvate, 2-oxoglutarate, oxaloacetate, and others. By comparing the concentration of intracellular metabolites in yeast and hyphal forms, nineteen intracellular metabolites were detected at higher concentrations in hyphae samples from all time points compared to yeast cells (Fig. 2). For example, aromatic amino acids such as phenylalanine and tyrosine increased their intracellular abundances during the yeast-to-hypha transition. The concentrations of fatty acids such as caprinate and

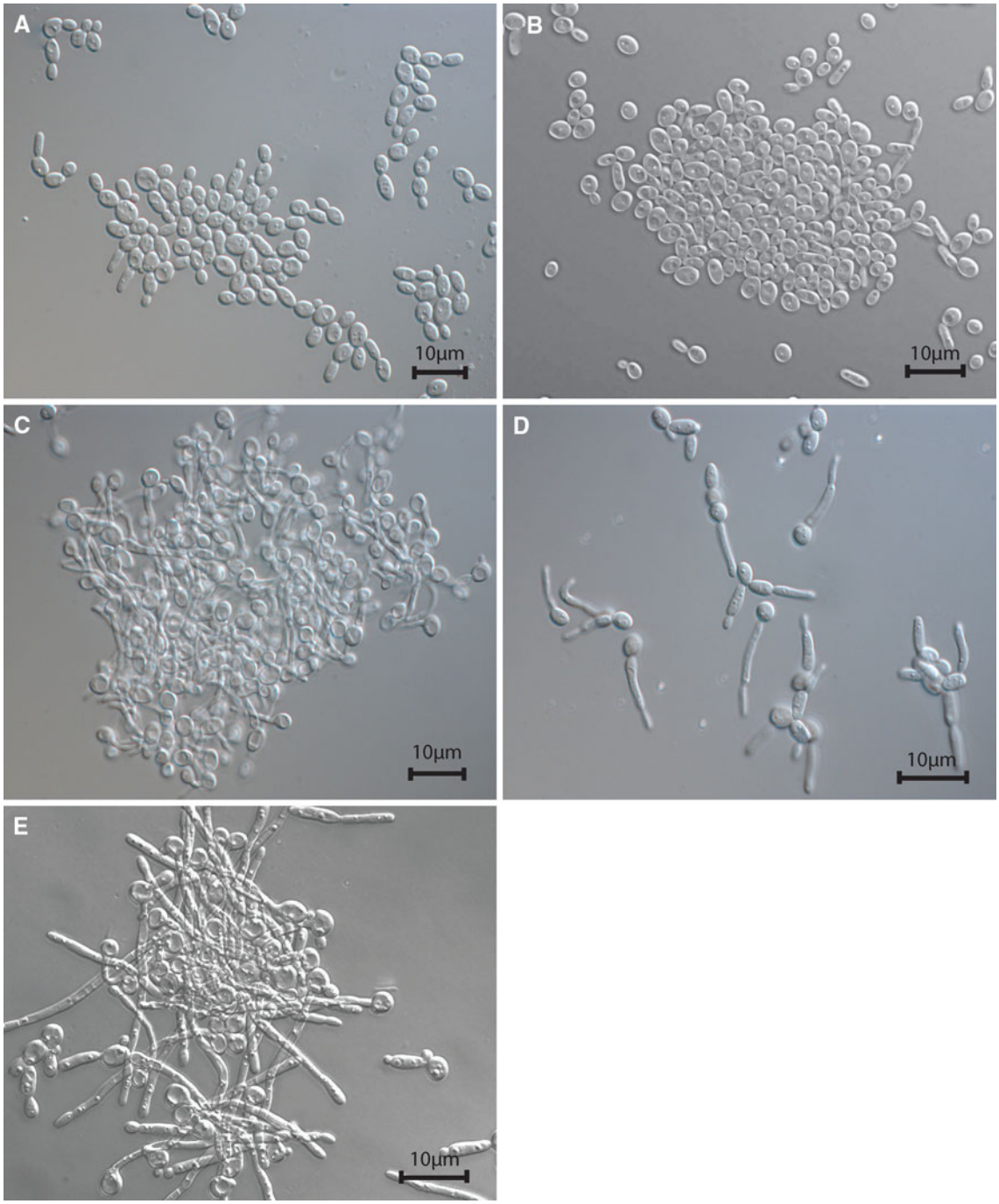

Fig. 1 The morphology of *C. albicans* cells incubated under different growth conditions at 37 °C for 3 h. **a** Minimum mineral medium (MM); **b** yeast peptone dextrose broth medium (YPD); **c** proline, *N*-acetylglucosamine medium (MPA); **d** Lee's medium; **e** serum medium. The *images* were taken by Nomarksi contrast microscopy with 100× magnification

myristate also increased during the morphological transition. The intracellular level of proline also increased in all hyphae-inducing conditions independently of the growth media. Interestingly, TCA cycle intermediates such malate and succinate were detected at higher intracellular levels in hyphal growth. By examining the intracellular metabolite profiles of yeast and hyphal cells over time, we observed a gradual increase in the global metabolite levels over the three hours of hyphal induction in comparison with yeast cells (Fig. 2). The higher concentration of intracellular metabolites during hyphal formation indicates that the flux through the respective pathway in which those metabolites play a part must have decreased in comparison to cells growing in the yeast form (Aggio et al. 2010), which

Table 1 Biomass and morphology of *C. albicans* cells cultured in different growth media

Media	Time					
	1 h		2 h		3 h	
	Biomass (mg/mL)	F (%)	Biomass (mg/mL)	F (%)	Biomass (mg/mL)	F (%)
MM	0.33	0	0.41	0	0.48	0
YPD	0.32	0	0.62	0	1.18	0
MPA	0.27	17	0.30	77	0.35	95
Serum	0.34	45	0.63	86	1.06	96
Lee's	0.39	51	0.66	94	1.14	99

MM minimum mineral medium; *YPD* yeast extract, peptone, dextrose medium; *MPA* minimum medium without glucose, supplemented with proline and *N*-acetylglucosamine; *F* percentage of filamentous growth determined by counting the number of yeast cells and filaments in 1 mm^3 volume

Table 2 Intracellular metabolites identified in *C. albicans* cells grown in different growth media

Classification of metabolites	No.	Intracellular metabolites
Amino acids and their isoforms	20	Alanine, asparagine, aspartate, cysteine, glutamine, glutamate, glycine, histidine, isoleucine, leucine, lysine, methionine, phenylalanine, proline, serine, threonine, tryptophan, tyrosine, valine, and β-alanine.
Amino acid derivatives	12	Adenosyl-L-methionine, creatinine, cystathionine, *N*-acetylglutamate, norleucine, norvaline, trans-4-hydroxyproline, ornithine, *S*-adenosyl-L-homocysteine, 2-aminobutyrate, δ-hydroxylysine, and pyroglutamate.
TCA cycle intermediates	7	Fumarate, citrate, succiniate, cis-aconitate, malate, 2-oxoglutarate, and oxaloacetate.
Fatty acids	12	Adipate, caprinate, caproate, caprylate, D-2-aminoadipate, L-2-amino-adipate, myristate, oleate, pentadecanoate, 14-methylpentadecanoate, stearate, and 3-hydroxyoctanoate.
Glycolytic intermediates	2	Pyruvate and phosphoenolpyruvate.
Cofactors and vitamins	3	NADP/NADPH, nicotinate, and 4-amino-*n*-butyrate.
Others	19	Benzoate, carbamate, citraconate, citramalate, hydroxybenzoate, glutarate, glycerate, itaconate, lactate, levulinate, malonate, phthalate, 2-isopropylmalate, 2-hydroxybutyrate, 10,13-dimethyltetradecanoate, 2,4-tert-butylphenol, 4-aminobenzoate, 3-methyl-2-oxopentanoate, and 10,12-octadecadienoate.
Total no. of identified metabolites	75	

directly reflects the altered metabolic states between yeast and hyphal cells. On the other hand, due to the different complexity of the three media used to induce hyphal formation, it was not possible to identify extracellular metabolites that consistently showed significant changes in concentration during morphogenesis in all hyphae-inducing media (data not shown). Therefore, we decided to focus our metabolomics study solely on the profile of intracellular metabolites.

3.3 Predicting metabolic pathway activities in *C. albicans* during the morphological transition

The profile of intracellular metabolites was used to compare the activity of metabolic pathways in *C. albicans* cells during the yeast-to-hypha transition. Surprisingly, we observed that the majority of the metabolic pathways were downregulated during this transition (Fig. 3). Although a few pathways were upregulated during the first hour of hyphal induction (e.g. fatty acid metabolism), almost all other metabolic pathways related to the metabolites detected in our samples were increasingly downregulated during morphogenesis. To further validate this observation, we quantified the total intracellular pool of ATP in cells from each growth condition. We found a significantly lower concentration of ATP in *C. albicans* cells growing under all hyphae-inducing conditions tested compared to cells growing as yeast (Fig. 4), which also indicates a global downregulation of cell primary (central carbon) metabolism in hyphal cells.

3.3.1 Metabolic changes most likely associated with morphogenesis

Since each hypha-inducing condition involved a different medium that was distinct from the media in which *C. albicans* grew in the yeast form, it is difficult to determine

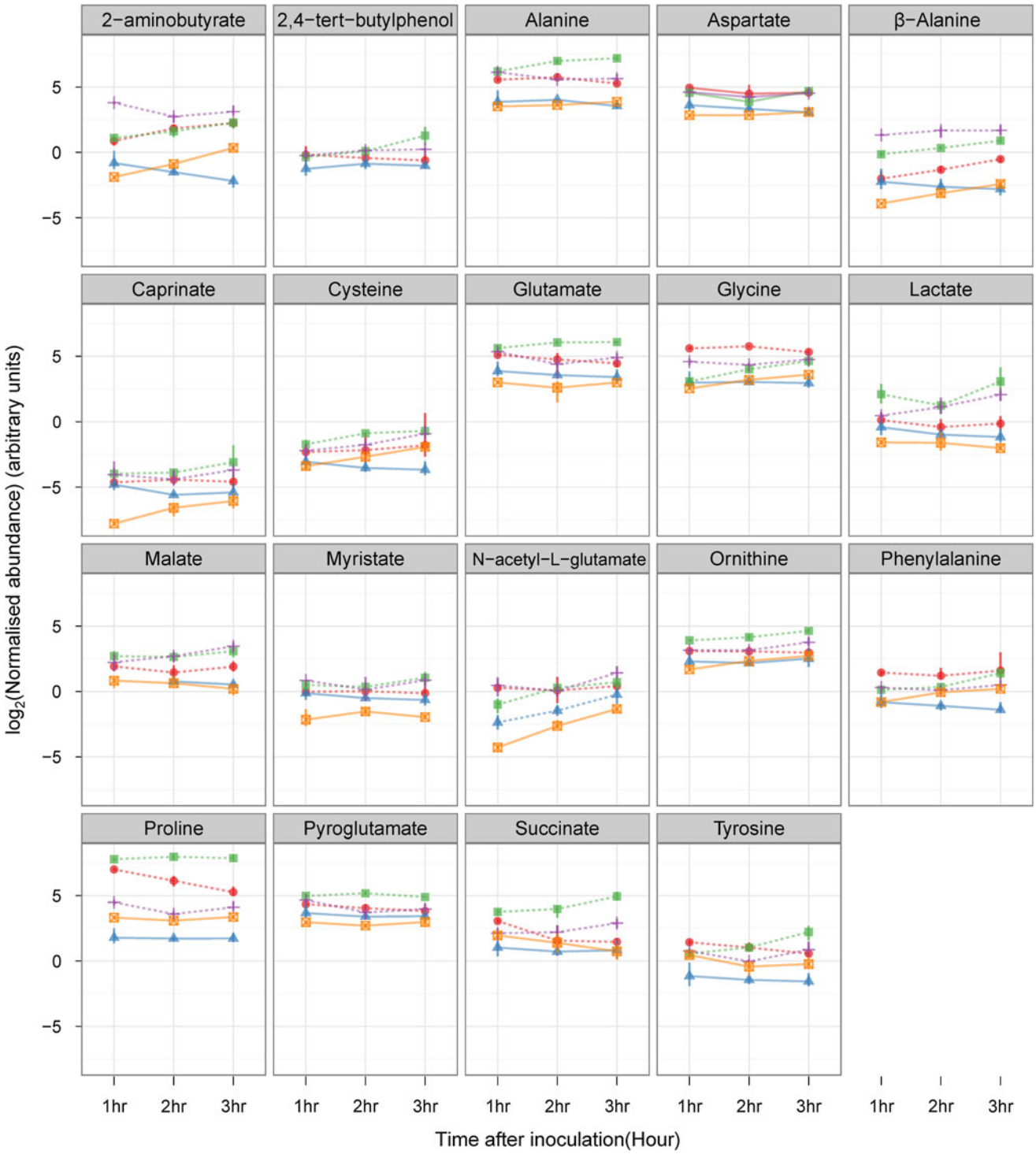

Fig. 2 Metabolite levels extracted from *C. albicans* cells cultured on different growth media. MM medium (▲); YPD medium (⊠); Lee's medium (●); MPA medium (■); and serum medium (+). The abundances of metabolites have been $\log_2$ transformed, and standard deviations are illustrated by *vertical line* ranges. Only the metabolites with statistically significant differences ($P < 0.05$) between both yeast (MM and YPD media) and all hyphal growth (MPA, serum, and Lee's media) are shown. *Missing lines* mean metabolite levels below detection limits (not-detected)

which metabolic pathway was changed due to the morphogenetic process *per se* rather than due to metabolism of different nutrients. Therefore, in order to identify metabolic changes most likely related to morphogenesis, we selected those metabolic pathways that showed significant differences during the yeast-to-hypha transition in all hyphae-inducing

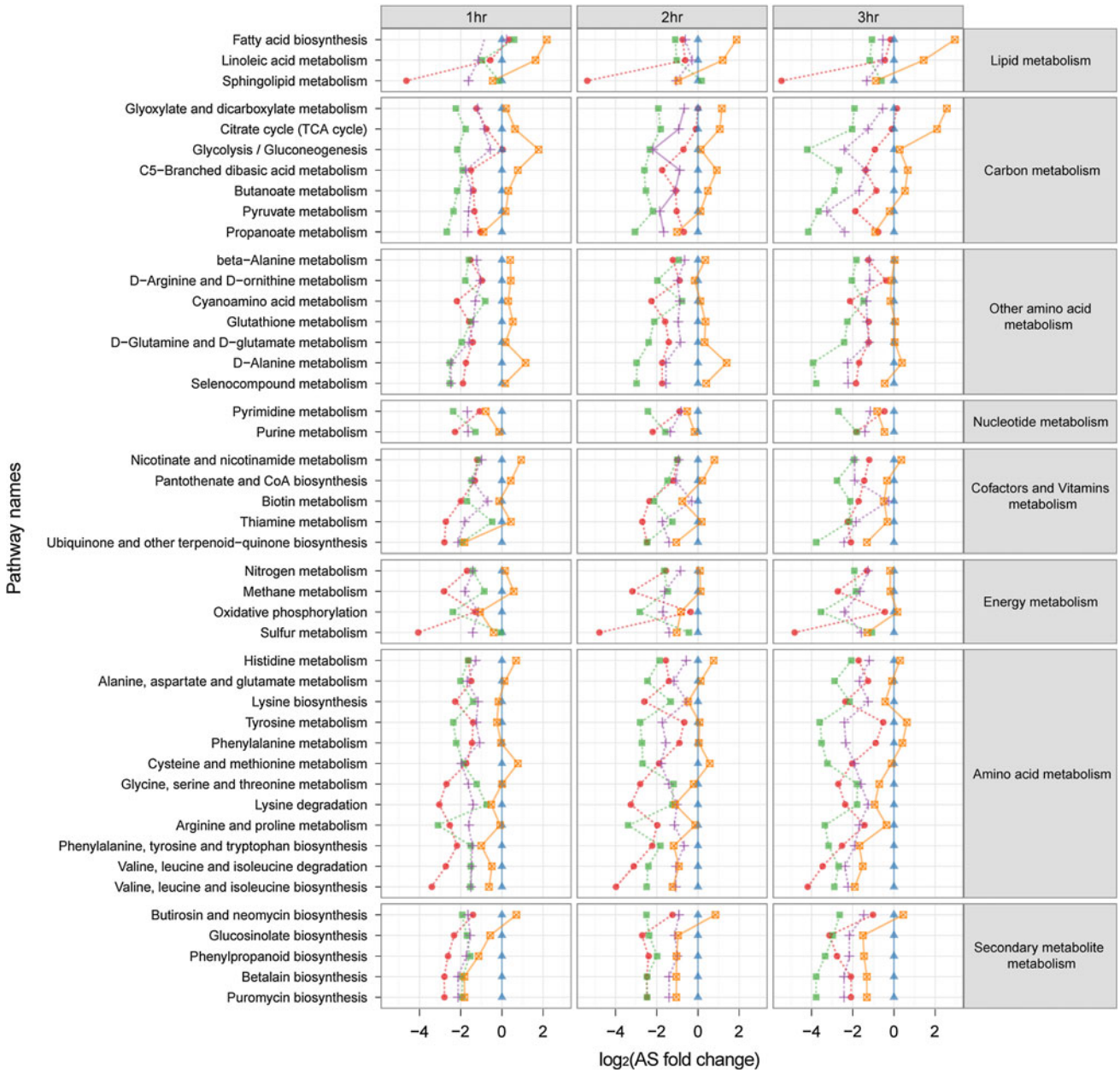

Fig. 3 Activities of *C. albicans* metabolic pathways based on intracellular metabolomic data from cells under different hypha-inducing conditions, at various time points, relative to the pathways in yeast cells. The activity scores (AS) for each pathway were calculated using our Pathway Activity Profiling (PAPi) algorithm (Aggio et al. 2010). PAPi calculates an AS for each metabolic pathway listed in KEGG database based on the number of metabolites identified from each pathway and their relative abundances. As a result, the AS represents the likelihood that a metabolic pathway is active in the cell and, consequently, allows the comparison of metabolic pathway activities using metabolite profile data. *C. albicans* were grown in the following media: (▲) MM medium; (⊠) YPD medium; (●) Lee's medium; (■) MPA medium; and (+) serum medium. Related pathways are grouped together according to their cellular metabolism and only pathways with statistically significant differences in activity ($P < 0.05$ by ANOVA) are shown

media across the three hours of incubation. Seventeen metabolic pathways appeared to have been downregulated in all three hypha-inducing conditions compared to yeast growth (Fig. 5). Thus, these pathways are likely to be associated with the morphogenesis of *C. albicans* because the transition from yeast to filamentous growth was the only common feature between these three growth conditions. Fourteen of the identified pathways were related to amino acid metabolism. Two pathways, CoA biosynthesis and arginine metabolism, have previously been implicated in the morphogenetic process occurring when *C. albicans* is engulfed by macrophages through transcriptomics and gene-knockout mutagenesis studies (Lorenz and Fink 2001; Ghosh et al. 2009). On the other hand, this is the first time that the downregulation of

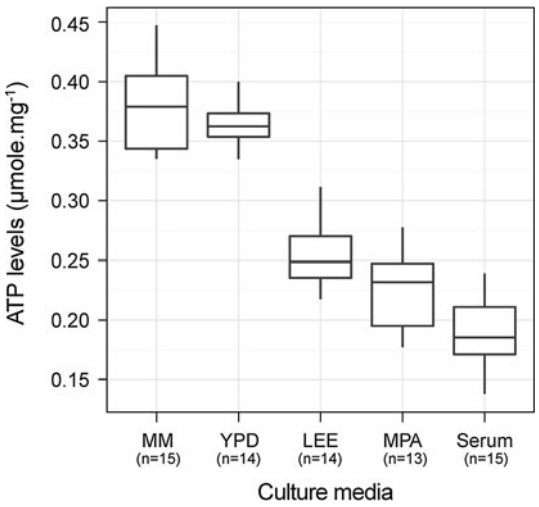

Fig. 4 ATP concentrations in *C. albicans* cells incubated under different growth conditions at 37 °C for 3 h. The ATP pool in cells grown under hypha-inducing conditions (*MPA* minimum proline *N*-acetylglucosamine medium, *LEE* Lee's medium, *Serum* 10 % bovine serum medium) were all significantly lower than those in cells grown as yeast in minimal mineral medium (MM) and yeast extract, peptone, dextrose broth (YPD) ($P < 0.001$)

nitrogen, nicotinate, and nicotinamide metabolism has been associated with *C. albicans* morphogenesis. Nitrogen metabolism not only serves to assimilate and excrete nitrogen-containing compounds, but it also maintains the balance between reduced and oxidized states of NADH, NADPH, and $FADH_2$. Nicotinate and nicotinamide metabolism produces NAD^+ through the recycling of compounds containing nicotinamide for the generation of NAD^+ and by de novo synthesis of NAD^+ from tryptophan or aspartate. Subsequently, NAD^+ is phosphorylated into $NADP^+$ by NAD^+ kinase (Lehninger 2005). These cofactors can affect the activity of many enzymes in the cell.

Integrating the seventeen downregulated metabolic pathways into a metabolic network enabled us to visualise the pathways connecting the central carbon metabolites detected in our samples (Fig. 6). The alanine asparate and glutamate metabolism, glycine serine and threonine metabolism, and arginine and proline metabolism appear to be the most connected pathways within the network. Furthermore, pyruvate, aspartate and glutamate could be considered as metabolite hubs linking all three pathways together during the morphogenetic process. Coincidently, glutamate and aspartate are also important intermediates in nitrogen metabolism since *C. albicans* can assimilate external ammonia into glutamate and through transamination to form aspartate. Thus, these metabolites act as key intermediates distributing nitrogen sources into different metabolic pathways. Moreover, the network demonstrates that aspartate, nicotinate, and fumarate may act as intermediary metabolites linking nicotinate and nicotinamide metabolism to other pathways. These metabolites could be important precursors for the biosynthesis of NADH and NADPH during *C. albicans* morphogenesis. Therefore, this metabolic network provides a framework that can guide the biological interpretation of metabolite profiles, and provide hypotheses to explain morphogenesis that can be tested in future studies.

4 Discussion

The general downregulation of cellular metabolism during the yeast-to-hypha transition was unexpected. Transcriptional upregulation of metabolic pathways seems to be the common trend during biofilm formation (García-Sánchez et al. 2004; Yeater et al. 2007), in which the majority of the cellular structures consist of filamentous forms. However, these biofilms were often sampled at 16 to 48 h after hyphal induction, when the cells had become established as a complex community. Besides, Montserrat et al. (2009) demonstrated that yeast cells, hyphae, and biofilms display different cytoplasmic protein profiles. Comparing yeast cells and hyphae, 67 of the 82 identified cytoplasmic proteins were less abundant in the hyphal form (Montserrat et al. 2009). Our metabolomic results confirm their findings, and we demonstrated that hyphae seem to be less metabolically active than yeast cells.

We have detected a significantly higher concentration of intracellular metabolites per dry weight of hyphal biomass than for yeast biomass (Fig. 2). Also, growth on serum and Lee's media resulted in a greater increase in *C. albicans* biomass (Table 1). Therefore, how could a global downregulation of metabolic pathways result in higher levels of intracellular metabolites and still present increased biomass production? Villas-Bôas et al. (2005b) showed that a higher concentration of intracellular metabolites does not always correlate with an increase in biomass. *S. cerevisiae* cells grown aerobically had a significantly lower concentration of intracellular metabolites and increased biomass production. Furthermore, in this study the *C. albicans* cultures growing on MPA medium (Table 1), also showed downregulation of most metabolic pathways despite showing just a small increase in biomass within three hours just like the control culture growing on MM in the yeast form. Therefore, the increased level of intracellular metabolites in *C. albicans* seems to be independent of the increase in biomass. Nonetheless, increases in intracellular metabolite levels could indicate a decrease in some biosynthetic activity due to the cells not using some metabolic intermediates, which is in agreement with a global downregulation of the central carbon metabolism. Furthermore, ATP is the key currency of intracellular energy transfer within biological systems, thus its concentration directly reflects the metabolic state of the central carbon metabolism.

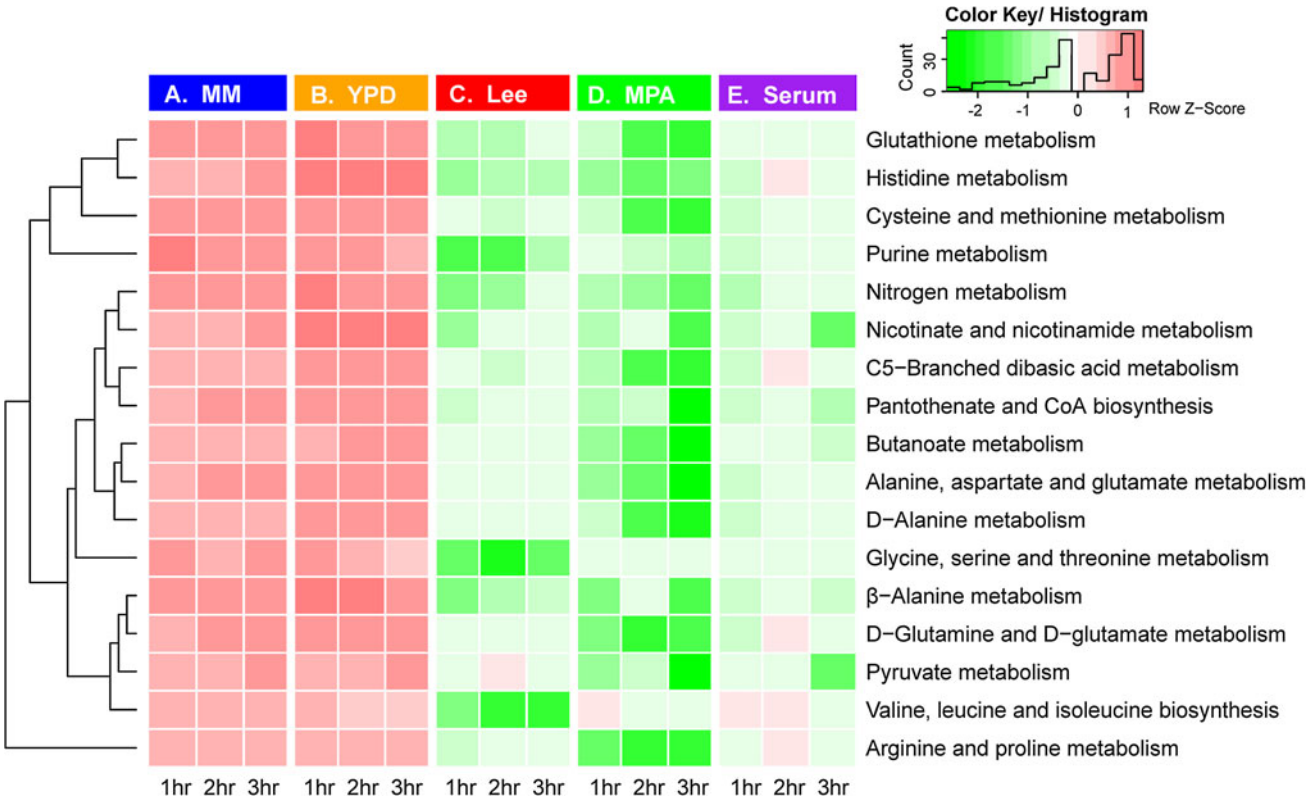

Fig. 5 Metabolic pathways consistently changed in all hyphal growth conditions. Only seventeen metabolic pathways showed significant differences in activity under all hypha-inducing conditions compared with the yeast growth at each of the time points. These metabolic pathways are involved in central carbon metabolism, which highlights the importance of primary metabolism in the regulation of hypha formation. The columns are separated according to growth medium: **a** MM medium (yeast growth); **b** YPD medium (yeast growth); **c** Lee's medium (hyphal growth); **d** MPA medium (hyphal growth); and **e** serum medium (hyphal growth). The *rows* list the metabolic pathways arranged according to hierarchical clustering analysis. The levels of metabolic pathway activities are indicated by *red* and *green* colour intensities. *Deeper red colours* indicate higher metabolic activities and *deeper green colours* mean lower metabolic activities. All metabolic activities have been centred in the *row direction* and scaled to have a mean of zero and a standard deviation of one (Row *Z* score). The *colour key* on the *top right* is superimposed by a histogram that counts all the metabolic activities (Color figure online)

Decrease in the ATP pool of a cell indicates a decrease in metabolic activity of the central carbon metabolism (Fig. 4), which correlates with our metabolomics results and PAPi hypotheses (Aggio et al. 2010).

We postulate that the prioritization of sugar metabolism in yeast cells is the underlying reason why yeast cells exhibit a higher level of central carbon metabolic activities than hyphae. The metabolism of sugars generates more energy for the cell to perform complex biosynthetic process. Therefore, when energy is available, macromolecules, such as proteins, lipids, and carbohydrates are easily synthesised (Walker 1998). Indeed, several studies indicate that in *C. albicans* the switch from yeast to hyphal growth is associated with the switch from aerobic to anaerobic respiration (Land et al. 1975; Aoki and Ito-kuwa 1982). The cells assimilate diverse alternative carbon sources in absence of glucose (Rubin-Bejerano et al. 2003; Lorenz et al. 2004; Fradin et al. 2005; Fernández-Arenas et al. 2007), which could be easier to be convert into certain hyphal macromolecules such as the biosynthesis of cell wall chitin directly from external *N*-acetylglucosamine. Therefore, hyphal growth could, indeed, be less metabolically (energetically) demanding to the fungal cells when growing in carbon or nitrogen poor environment or under anaerobiosis.

Thus, we hypothesise that once the metabolic activity of yeast cells is temporarily disrupted by environmental changes, such as starvation, stress, alkaline pH, depletion in oxygen and high temperatures, the central carbon metabolism of *C. albicans* is globally downregulated. This downregulation of the central carbon metabolism triggers changes to a growth form that demands less energy. This explains why *C. albicans* undergoes hypha formation when it is starved for several hours and then exposed to poor carbon or nitrogen sources (Holmes and Shepherd 1987, 1988). Moreover, *C. albicans* yeast cells that colonize host mucosa and epithelial surfaces will be in an environment where glucose is scarce, but complex carbohydrates

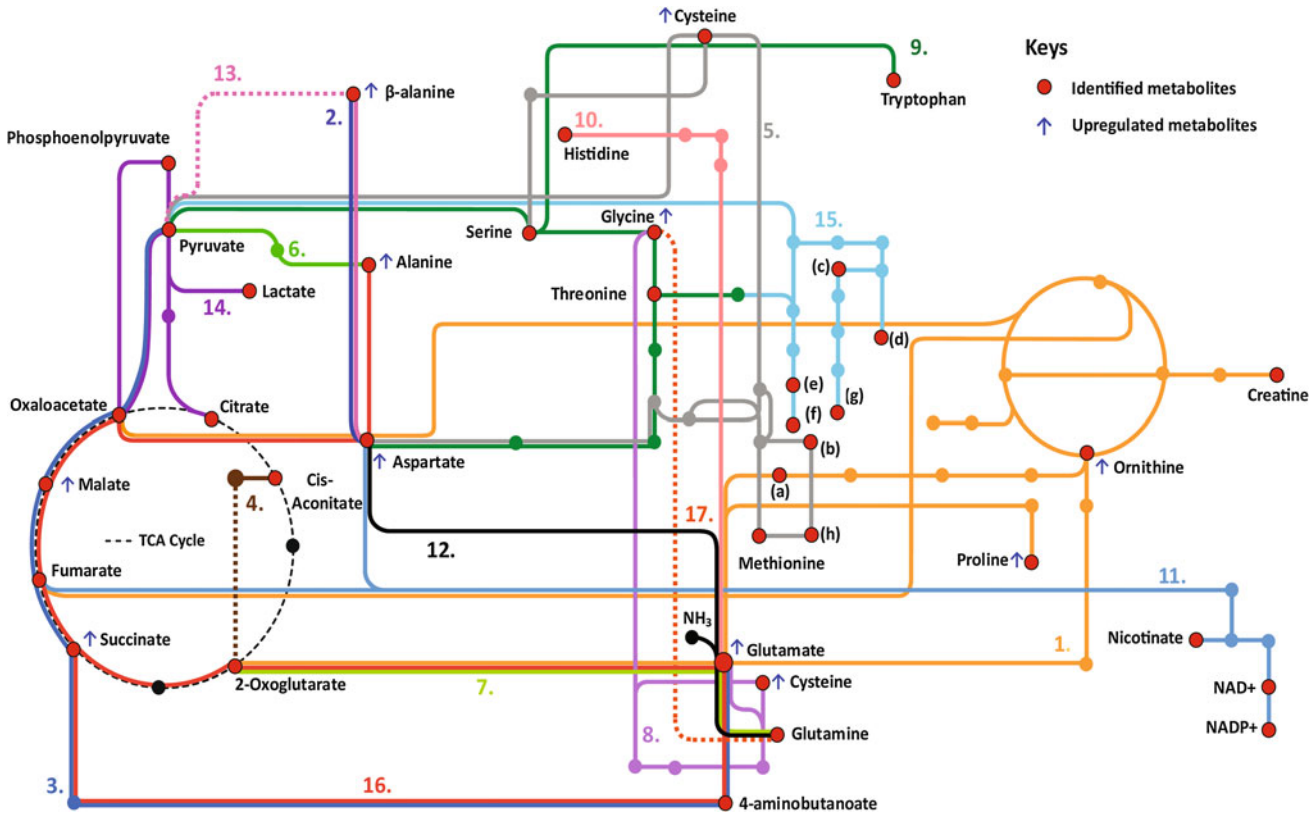

Fig. 6 Metabolic network illustrating how the seventeen morphogenesis-related metabolic pathways (Fig. 4) are interconnected. Metabolic pathways have been connected via identified metabolites represented by *red dots*. *Blue arrows* indicate that the metabolites were detected at a higher level in hyphal growth. *Dashed lines* indicate multiple hidden steps in that pathway. The names of the pathway are as follow: (*1*) arginine and proline metabolism, (*2*) *β*-alanine metabolism, (*3*) butanoate metabolism, (*4*) C5 branched dibasic acid metabolism, (*5*) cysteine and methionine metabolism, (*6*) D-alanine metabolism, (*7*) D-glutamine and D-glutamate metabolism, (*8*) glutathione metabolism, (*9*) glycine, serine and threonine metabolism, (*10*) histidine metabolism, (*11*) nicotinate and nicotinamide metabolism, (*12*) nitrogen metabolism, (*13*) pantothenate and CoA biosynthesis, (*14*) pyruvate metabolism, (*15*) valine, leucine and isoleucine biosynthesis, (*16*) alanine, aspartate and glutamate metabolism, and (*17*) purine metabolism. The metabolites labelled by letters are: (*a*) *N*-acetyl-L-glutamate; (*b*) *S*-adensyl-L-homocystein; (*c*) 2-isopropylmalate; (*d*) valine; (*e*) *S*-3-methyl-2-oxopentanoate; (*f*) isoleucine; (*g*) leucine; and (*h*) *S*-adenosyl-L-methionine (Color figure online)

proteins and lipids are present. Such cells often form hyphae and penetrate the epithelia.

On the other hand, linking our metabolomics data to pre-existing transcriptomics and proteomics data on morphogenesis of *C. albicans* has presented a challenge. Although there are many transcriptomics and proteomics studies that have examined *C. albicans* morphogenesis, the majority of the studies has utilised mutants with deleted or overexpressed genes involved in signalling cascades or encoding transcriptional regulators (Murad et al. 2001; Bensen et al. 2004; Doedt et al. 2004; Yin et al. 2004; García-Sánchez et al. 2005; Tournu et al. 2005; Enjalbert et al. 2006; Zacchi et al. 2010; Stichternoth et al. 2011). The disruption of any of these genes would interfere not only with morphogenesis, but also with many other essential cellular processes. Recently, Monteoliva et al. (2011) investigated the proteome profiles of *C. albicans* yeast and hyphal cells using Lee's medium at pH 4.3 or 6.6 to obtain yeast or hyphal forms, respectively. This means that it is uncertain whether changes in protein levels were the consequence of different pH conditions or morphogenesis. However, they revealed a significantly lower amount of cytosolic proteins in hyphae involved in respiration, the pentose phosphate pathway, and biosynthetic pathways for vitamins, cofactors, purines, nucleotides, glutamate, isoleucine, leucine, and valine. These results are in general agreement with our findings. In addition, the emphasis placed by the authors on the downregulation of redox processes during hypha formation also supports our findings. Here, we have shown that the cellular metabolism of nitrogen, and nicotinate and nicotinamide were all downregulated while *C. albicans* was growing under hyphal-inducing conditions. These pathways are known to play an important role in the oxidative-reduction processes of the cell.

5 Conclusions

In this study, we have used metabolomics to present evidence of global metabolic changes in the central carbon metabolism of *C. albicans* during the yeast-to-hypha morphological transition. We have observed a global downregulation of cellular metabolism during hypha formation. These results highlight the importance of the regulation of central carbon metabolism in the morphogenesis of *C. albicans*, as an immediate downstream response to environmental signals. Therefore, the current understanding of morphogenesis can be further elucidated by investigating the key central carbon metabolic pathways identified in this study.

Acknowledgments We thank D. Wagachchi for assisting with sample preparation; and R. Aggio and L. Fearnley for data analysis assistance. This work was supported by Faculty of Science Research Funding, University of Auckland and by the University of Auckland Doctoral Scholarship for Ting-Li Han.

References

Aggio, R. B. M., Ruggiero, K., & Villas-Bôas, S. G. (2010). Pathway activity profiling (papi): From the metabolite profile to the metabolic pathway activity. *Bioinformatics, 26*, 2969–2976.

Aoki, S., & Ito-kuwa, S. (1982). Respiration of *Candida albicans* in relation to its morphogenesis. *Plant and Cell Physiology, 23*, 721–726.

Arai, T., Mikami, Y., & Yokoyama, K. (1977). Phagocytosis of *Candida albicans* by rabbit alveolar macrophages and guinea pig neutrophils. *Sabouraudia Journal of Medical and Veterinary Mycology, 15*, 171–177.

Banerjee, M., Thompson, D. S., Lazzell, A., Carlisle, P. L., Pierce, C., Monteagudo, C., et al. (2008). UME6, a novel filament-specific regulator of *Candida albicans* hyphal extension and virulence. *Molecular Biology of the Cell, 19*, 1354–1365.

Bendel, C. M., Hess, D. J., Garni, R. M., Henry-Stanley, M., & Wells, C. L. (2003). Comparative virulence of *Candida albicans* yeast and filamentous forms in orally and intravenously inoculated mice. *Critical Care Medicine, 31*, 501–507.

Bensen, E. S., Martin, S. J., Li, M., Berman, J., & Davis, D. A. (2004). Transcriptional profiling in *Candida albicans* reveals new adaptive responses to extracellular pH and functions for Rim101p. *Molecular Microbiology, 54*, 1335–1351.

Braun, B. R., & Johnson, A. D. (1997). Control of filament formation in *Candida albicans* by the transcriptional repressor TUP1. *Science, 277*, 105–109.

Brown, D. H., Jr, Giusani, A. D., Chen, X., & Kumamoto, C. A. (1999). Filamentous growth of *Candida albicans* in response to physical environmental cues and its regulation by the unique CZF1 gene. *Molecular Microbiology, 34*, 651–662.

Carman, A. J., Vylkova, S., & Lorenz, M. C. (2008). Role of acetyl coenzyme a synthesis and breakdown in alternative carbon source utilization in *Candida albicans*. *Eukaryotic Cell, 7*, 1733–1741.

Chen, H., Fujita, M., Feng, Q., Clardy, J., & Fink, G. R. (2004). Tyrosol is a quorum-sensing molecule in *Candida albicans*. *Proceedings of the National academy of Sciences of the United States of America, 101*, 5048–5052.

Cheng, G., Yeater, K. M., & Hoyer, L. L. (2006). Cellular and molecular biology of *Candida albicans* estrogen response. *Eukaryotic Cell, 5*, 180–191.

Doedt, T., Krishnamurthy, S., Bockmühl, D. P., Tebarth, B., Stempel, C., Russell, C. L., et al. (2004). APSES proteins regulate morphogenesis and metabolism in *Candida albicans*. *Molecular Biology of the Cell, 15*, 3167–3180.

Eisman, B., Alonso-Monge, R., Román, E., Arana, D., Nombela, C., & Pla, J. (2006). The Cek1 and Hog1 mitogen-activated protein kinases play complementary roles in cell wall biogenesis and chlamydospore formation in the fungal pathogen *Candida albicans*. *Eukaryotic Cell, 5*, 347–358.

Enjalbert, B., Smith, D. A., Cornell, M. J., Alam, I., Nicholls, S., Brown, A. J. P., et al. (2006). Role of the Hog1 stress-activated protein kinase in the global transcriptional response to stress in the fungal pathogen *Candida albicans*. *Molecular Biology of the Cell, 17*, 1018–1032.

Feng, Q., Summers, E., Guo, B., & Fink, G. (1999). Ras signaling is required for serum-induced hyphal differentiation in *Candida albicans*. *Journal of Bacteriology, 181*, 6339–6346.

Fernández-Arenas, E., Cabezón, V., Bermejo, C., Arroyo, J., Nombela, C., Diez-Orejas, R., et al. (2007). Integrated proteomics and genomics strategies bring new insight into *Candida albicans* response upon macrophage interaction. *Molecular and Cellular Proteomics, 6*, 460–478.

Fradin, C., De Groot, P., MacCallum, D., Schaller, M., Klis, F., Odds, F. C., et al. (2005). Granulocytes govern the transcriptional response, morphology and proliferation of *Candida albicans* in human blood. *Molecular Microbiology, 56*, 397–415.

García-Sánchez, S., Aubert, S., Iraqui, I., Janbon, G., Ghigo, J. M., & D'Enfert, C. (2004). *Candida albicans* biofilms: A developmental state associated with specific and stable gene expression patterns. *Eukaryotic Cell, 3*, 536–545.

García-Sánchez, S., Mavor, A. L., Russell, C. L., Argimon, S., Dennison, P., Enjalbert, B., et al. (2005). Global roles of Ssn6 in tup1- And nrg1-dependent gene regulation in the fungal pathogen, *Candida albicans*. *Molecular Biology of the Cell, 16*, 2913–2925.

Ghosh, S., Navarathna, D. H. M. L. P., Roberts, D. D., Cooper, J. T., Atkin, A. L., Petro, T. M., et al. (2009). Arginine-induced germ tube formation in *Candida albicans* is essential for escape from murine macrophage line RAW 264.7. *Infection and Immunity, 77*, 1596–1605.

Gillum, A. M., Tsay, E. Y. H., & Kirsch, D. R. (1984). Isolation of the *Candida albicans* gene for orotidine-5′-phosphate decarboxylase by complementation of *S. cerevisiae* ura3 and *E. coli* pyrF mutations. *Molecular and General Genetics, 198*, 179–182.

Han, T. L., Cannon, R. D., & Villas-Bôas, S. G. (2011). The metabolic basis of *Candida albicans* morphogenesis and quorum sensing. *Fungal Genetics and Biology, 48*(8), 747–763.

Hogan, D. A., Vik, A., & Kolter, R. (2004). A *Pseudomonas aeruginosa* quorum-sensing molecule influences *Candida albicans* morphology. *Molecular Microbiology, 54*, 1212–1223.

Holmes, A. R., & Shepherd, M. G. (1987). Proline-induced germ-tube formation in *Candida albicans*: Role of proline uptake and nitrogen metabolism. *Journal of General Microbiology, 133*, 3219–3228.

Holmes, A. R., & Shepherd, M. G. (1988). Nutritional factors determine germ tube formation in *Candida albicans*. *Journal of Medical and Veterinary Mycology, 26*, 127–131.

Hornby, J. M., Jensen, E. C., Lisec, A. D., Tasto, J. J., Jahnke, B., Shoemaker, R., et al. (2001). Quorum sensing in the dimorphic fungus *Candida albicans* is mediated by farnesol. *Applied and Environmental Microbiology, 67*, 2982–2992.

Hwang, C. S., Oh, J. H., Huh, W. K., Yim, H. S., & Kang, S. O. (2003). Ssn6, an important factor of morphological conversion

and virulence in *Candida albicans*. *Molecular Microbiology, 47*, 1029–1043.

José, C. S., Monge, R. A., Pérez-Díaz, R., Pla, J., & Nombela, C. (1996). The mitogen-activated protein kinase homolog HOG1 gene controls glycerol accumulation in the pathogenic fungus *Candida albicans*. *Journal of Bacteriology, 178*, 5850–5852.

Kadosh, D., & Johnson, A. D. (2001). Rfg1, a protein related to the *Saccharomyces cerevisiae* hypoxic regulator Rox1, controls filamentous growth and virulence in *Candida albicans*. *Molecular and Cellular Biology, 21*, 2496–2505.

Kell, D. B., Brown, M., Davey, H. M., Dunn, W. B., Spasic, I., & Oliver, S. G. (2005). Metabolic footprinting and systems biology: The medium is the message. *Nature Reviews Microbiology, 3*, 557–565.

Kresnowati, M. T., van Winden, W. A., Almering, M. J., ten Pierick, A., Ras, C., Knijnenburg, T. A., et al. (2006). When transcriptome meets metabolome: Fast cellular responses of yeast to sudden relief of glucose limitation. *Molecular Systems Biology [electronic resource], 2*, 49.

Land, G. A., McDonald, W. C., Stjernholm, R. L., & Friedman, L. (1975). Factors affecting filamentation in *Candida albicans*: Changes in respiratory activity of *Candida albicans* during filamentation. *Infection and Immunity, 12*, 119–127.

Lee, K. L., Buckley, H. R., & Campbell, C. C. (1975). An amino acid liquid synthetic medium for the development of mycelial and yeast forms of *Candida albicans*. *Sabouraudia Journal of Medical and Veterinary Mycology, 13*, 148–153.

Lehninger, A. L. (2005). *Lehninger principles of biochemistry*. New York: W.H. Freeman.

Lingappa, B. T., Prasad, M., Lingappa, Y., Hunt, D. F., & Biemann, K. (1969). Phenethyl alcohol and tryptophol: Autoantibiotics produced by the fungus *Candida albicans*. *Science, 163*, 192–194.

Lo, H. J., Köhler, J. R., Didomenico, B., Loebenberg, D., Cacciapuoti, A., & Fink, G. R. (1997). Nonfilamentous *C. albicans* mutants are avirulent. *Cell, 90*, 939–949.

Lorenz, M. C., & Fink, G. R. (2001). The glyoxylate cycle is required for fungal virulence. *Nature, 412*, 83–86.

Lorenz, M. C., Bender, J. A., & Fink, G. R. (2004). Transcriptional response of *Candida albicans* upon internalization by macrophages. *Eukaryotic Cell, 3*, 1076–1087.

Maidan, M. M., De Rop, L., Serneels, J., Exler, S., Rupp, S., Tournu, H., et al. (2005a). The G protein-coupled receptor Gpr1 and the Gα protein Gpa2 act through the cAMP-protein kinase A pathway to induce morphogenesis in *Candida albicans*. *Molecular Biology of the Cell, 16*, 1971–1986.

Maidan, M. M., Thevelein, J. M., & Van Dijck, P. (2005b). Carbon source induced yeast-to-hypha transition in *Candida albicans* is dependent on the presence of amino acids and on the G-protein-coupled receptor Gpr1. *Biochemical Society Transactions, 33*, 291–293.

Monteoliva, L., Martinez-Lopez, R., Pitarch, A., Hernaez, M. L., Serna, A., Nombela, C., et al. (2011). Quantitative proteome and acidic subproteome profiling of *Candida albicans* yeast-to-hypha transition. *Journal of Proteome Research, 10*, 502–517.

Montserrat, M.-G., Perumal, P., Mekala, S., Nombela, C., Chaffin, W. L., & Gil, C. (2009). Proteomic analysis of cytoplasmic and surface proteins from yeast cells, hyphae, and biofilms of *Candida albicans*. *Proteomics, 9*, 2230–2252.

Murad, A. M. A., D'Enfert, C., Gaillardin, C., Tournu, H., Tekaia, F., Talibi, D., et al. (2001). Transcript profiling in *Candida albicans* reveals new cellular functions for the transcriptional repressors CaTup1, CaMig1 and CaNrg1. *Molecular Microbiology, 42*, 981–993.

Nickerson, K. W., Atkin, A. L., & Hornby, J. M. (2006). Quorum sensing in dimorphic fungi: Farnesol and beyond. *Applied and Environmental Microbiology, 72*, 3805–3813.

Oh, K. B., Miyazawa, H., Naito, T., & Matsuoka, H. (2001). Purification and characterization of an autoregulatory substance capable of regulating the morphological transition in *Candida albicans*. *Proceedings of the National academy of Sciences of the United States of America, 98*, 4664–4668.

Pedreño, Y., Maicas, S., Argüelles, J. C., Sentandreu, R., & Valentin, E. (2004). The ATC1 gene encodes a cell wall-linked acid trehalase required for growth on trehalose in *Candida albicans*. *Journal of Biological Chemistry, 279*, 40852–40860.

Prigneau, O., Porta, A., & Maresca, B. (2004). *Candida albicans* CTN gene family is induced during macrophage infection: Homology, disruption and phenotypic analysis of CTN3 gene. *Fungal Genetics and Biology, 41*, 783–793.

Raamsdonk, L. M., Teusink, B., Broadhurst, D., Zhang, N., Hayes, A., Walsh, M. C., et al. (2001). A functional genomics strategy that uses metabolome data to reveal the phenotype of silent mutations. *Nature Biotechnology, 19*, 45–50.

Reynolds, R., & Braude, A. I. (1956). The filament inducing property of blood for *Candida albicans*; its nature and significance. *Clinical Research Procedure, 4*, 40.

Romani, L., Bistoni, F., & Puccetti, P. (2003). Adaptation of *Candida albicans* to the host environment: The role of morphogenesis in virulence and survival in mammalian hosts. *Current Opinion in Microbiology, 6*, 338–343.

Rooney, P. J., & Klein, B. S. (2002). Linking fungal morphogenesis with virulence. *Cellular Microbiology, 4*, 127–137.

Rubin-Bejerano, I., Fraser, I., Grisafi, P., & Fink, G. R. (2003). Phagocytosis by neutrophils induces an amino acid deprivation response in *Saccharomyces cerevisiae* and *Candida albicans*. *Proceedings of the National academy of Sciences of the United States of America, 100*, 11007–11012.

Saville, S. P., Lazzell, A. L., Monteagudo, C., & Lopez-Ribot, J. L. (2003). Engineered control of cell morphology in vivo reveals distinct roles for yeast and filamentous forms of *Candida albicans* during infection. *Eukaryotic Cell, 2*, 1053–1060.

Schweizer, A., Rupp, S., Taylor, B. N., Röllinghoff, M., & Schröppel, K. (2000). The TEA/ATTS transcription factor CaTec1p regulates hyphal development and virulence in *Candida albicans*. *Molecular Microbiology, 38*, 435–445.

Singh, V., Satheesh, S. V., Raghavendra, M. L., & Sadhale, P. P. (2007). The key enzyme in galactose metabolism, UDP-galactose-4-epimerase, affects cell-wall integrity and morphology in *Candida albicans* even in the absence of galactose. *Fungal Genetics and Biology, 44*, 563–574.

Smart, K. F., Aggio, R. B. M., Van Houtte, J. R., & Villas-Bôas, S. G. (2010). Analytical platform for metabolome analysis of microbial cells using methyl chloroformate derivatization followed by gas chromatography-mass spectrometry. *Nature Protocols, 5*, 1709–1729.

Stichternoth, C., Fraund, A., Setiadi, E., Giasson, L., Vecchiarelli, A., & Ernst, J. F. (2011). Sch9 kinase integrates hypoxia and CO2 sensing to suppress hyphal morphogenesis in *Candida albicans*. *Eukaryotic Cell, 10*, 502–511.

Stoldt, V. R., Sonneborn, A., Leuker, C. E., & Ernst, J. F. (1997). Efg1p, an essential regulator of morphogenesis of the human pathogen *Candida albicans*, is a member of a conserved class of bHLH proteins regulating morphogenetic processes in fungi. *EMBO Journal, 16*, 1982–1991.

Strijbis, K., Van Roermund, C. W. T., Visser, W. F., Mol, E. C., Van Den Burg, J., MacCallum, D. M., et al. (2008). Carnitine-dependent transport of acetyl coenzyme A in *Candida albicans* is essential for growth on nonfermentable carbon sources and contributes to biofilm formation. *Eukaryotic Cell, 7*, 610–618.

Tournu, H., Tripathi, G., Bertram, G., Macaskill, S., Mavor, A., Walker, L., et al. (2005). Global role of the protein kinase Gcn2

in the human pathogen *Candida albicans*. *Eukaryotic Cell, 4*, 1687–1696.

Tripathi, G., Wiltshire, C., Macaskill, S., Tournu, H., Budge, S., & Brown, A. J. P. (2002). Gcn4 co-ordinates morphogenetic and metabolic responses to amino acid starvation in *Candida albicans*. *EMBO Journal, 21*, 5448–5456.

Verduyn, C., Postma, E., Scheffers, W. A., & Van Dijken, J. P. (1992). Effect of benzoic acid on metabolic fluxes in yeasts: A continuous-culture study on the regulation of respiration and alcoholic fermentation. *Yeast, 8*, 501–517.

Villas-Bôas, S. G., Åkesson, M., & Nielsen, J. (2005a). Biosynthesis of glyoxylate from glycine in *Saccharomyces cerevisiae*. *FEMS Yeast Research, 5*, 703–709.

Villas-Bôas, S. G., Mas, S., Åkesson, M., Smedsgaard, J., & Nielsen, J. (2005b). Mass spectrometry in metabolome analysis. *Mass Spectrometry Reviews, 24*, 613–646.

Villas-Bôas, S. G., Roessner, U., Hansen, M. A. E., Smedsfaard, J., & Nielsen, J. (2007). *Metabolome analysis: An introduction*. New Jersey: Wiley-Interscience.

Visser, D., Van Zuylen, G. A., Van Dam, J. C., Eman, M. R., Pröll, A., Ras, C., et al. (2004). Analysis of in vivo kinetics of glycolysis in aerobic *Saccharomyces cerevisiae* by application of glucose and ethanol pulses. *Biotechnology and Bioengineering, 88*, 157–167.

Walker, G. M. (1998). *Yeast physiology and biotechnology*. Chichester: Wiley-Blackwell.

Yeater, K. M., Chandra, J., Cheng, G., Mukherjee, P. K., Zhao, X., Rodriguez-Zas, S. L., et al. (2007). Temporal analysis of *Candida albicans* gene expression during biofilm development. *Microbiology, 153*, 2373–2385.

Yin, Z., Stead, D., Selway, L., Walker, J., Riba-Garcia, I., McInerney, T., et al. (2004). Proteomic response to amino acid starvation in *Candida albicans* and *Saccharomyces cerevisiae*. *Proteomics, 4*, 2425–2436.

Zacchi, L. F., Gomez-Raja, J., & Davis, D. A. (2010). Mds3 regulates morphogenesis in *Candida albicans* through the TOR pathway. *Molecular and Cellular Biology, 30*, 3695–3710.

Zaragoza, O., Blazquez, M. A., & Gancedo, C. (1998). Disruption of the *Candida albicans* TPS1 gene encoding trehalose-6-phosphate synthase impairs formation of hyphae and decreases infectivity. *Journal of Bacteriology, 180*, 3809–3815.

Zhou, H., & Lorenz, M. C. (2008). Carnitine acetyltransferases are required for growth on non-fermentable carbon sources but not for pathogenesis in *Candida albicans*. *Microbiology, 154*, 500–509.